Characterization and Responsivity of Graphene Loaded Zinc Sulphide within Visible Light Spectrum

Sabreen A. Khalaf[1*] and Iftikhar M. Ali[2]

[1,2]*Dept. of Phys., College of science, Baghdad University.*

ABSTRACT

In this study, the nanocrystal-ZnS-loaded graphene was synthesized by a facile co-precipitation route. The effect of graphene on the characterization of Zinc Sulphide (ZnS) was investigated. The X-ray Diffraction (XRD) results reveal that ZnS has cubic system while hexagonal structure which is observed by loading graphene during the preparation of ZnS. Energy Dispersive X-ray Spectroscopy (EDS) analysis proved the presence of all expected elements in the prepared materials. Nanosize of fabricated materials has been measured using Scanning Electron Microscopy (SEM) technique. This study also found that the graphene plays a critical role in lowering the optical energy gap of ZnS nanoparticles from 4 eV to 3.2 eV. The characterization of detector fabricated from these materials showed that the ZnS/graphene nanostructure exhibits colour tuneable to green region compared to bare ZnS which has responsivity at blue region, due to the addition of graphene.

Keywords: ZnS, Graphene, Nanocrystals, Composites, Detectors.

1. INTRODUCTION

Almost all materials system including metal, insulators and semiconductors are size dependent electronic or optical properties in the quantum size regime. Among those properties, the modification in the energy band gap of semiconductors is the most attractive properties due to the fundamental and technological importance [1]. Semiconductors with widely tuneable energy band gap are considered to be the materials for next-generation flat panel displays, photovoltaic, optoelectronic devices, laser, sensors, and, photonic bandgap devices.

Zinc Sulphide (ZnS) is one of the first semiconductors discovered and an important semiconductor material with direct wide band gaps for cubic and hexagonal phases of 3.72 and 3.77 eV, respectively. It has a high absorption coefficient in the visible range of the optical spectrum and reasonably good electrical properties. Furthermore, ZnS semiconductor materials have a wide range of applications such as in electroluminescence devices, phosphors, light-emitting displays, and optical sensors [2-6].

A single layer of graphene is called Graphene Nanosheet (GNS), which has a wide range of unique physical features: 2-dimensional planar structure, zero band gap, half-metallicity, and high electron mobility. Due to electronic properties and its structure, the GNS is promising in various applications such as nanoelectronics, solid-state sensors, and, spintronic [7-10].

*Corresponding Author: *sabreenali850@yahoo.com*

Photoconductivity (PC) is defined as electrical conductivity resulting from photo-induced electron excitations in which light is absorbed. In semiconductors, PC arises due to the interaction of photons with bound electrons of lattice atoms that leads to photo-generation of electron-hole pairs after the absorption of photons, hence, increases carrier density and conductivity of material [11,12]. Extensive study of photoconductivity has been made in nanoparticles, thin film, nanorods, nanowires, and mixed lattice for different parameters [13,14].

This work studied the effect of graphene nanosheet on the responsivity of zinc sulphide and presents the characterization of ZnS and ZnS/Gr.

2. EXPERIMENTAL DETAILS

ZnS nanoparticles were synthesized by co-precipitation chemical method. In a typical way to approach stoichiometric structure for zinc sulphide, a stock solution of Zn^{2+} was prepared by adding 0.1 M of $Zn(NO_3)_2.6H_2O$ into 50mL of distilled water. A stock solution of S^{2-} was prepared by adding 0.2 M of Na_2S into 50mL of distilled water. Then the first solution was placed on a magnetic stirrer at a temperature of 80°C for 1 hour. Then, the second solution is added to the first solution dropwise and the whole solution is stirred for 30 minutes. Then, the resultant compound obtained was filtered and washed several times using distilled water, ethanol and finally by acetone. The compound was then dried using the oven at 100°C for 5 hours.

For preparing ZnS/graphene, 0.1 g of graphene nanosheets purchased from Sigma Aldrich is weighted and stirred with DMF solution for 6 hours, then sonicated for another 6 hours to get a homogeneous suspension. An appropriate volume of Gr suspension was added to a stock solution of Zn^{2+} and stirred together at 80°C for 1 hour, and the same procedure was repeated. The resultant powders were characterized by X-ray Diffraction (XRD), Energy Dispersive X-ray Spectroscopy (EDS), and Scanning Electron Microscopy (SEM) analysis.

Thin films are prepared by a spin coating technique. For thin films preparation, 10 mg from the powder of ZnS or ZnS/Gr was dissolved in 10 ml of distilled water and left it overnight to fully dissolve. Then, the solution was sonicated in an ultrasonic bath for 30 minutes before spin coating process. Finally, the solution was spin-coated on substrates by a spin coater at a speed of 2000 rpm and was repeated for 5 times in order to obtain a homogeneous thin film and achieve the required thickness. The substrate was placed in an oven at 100°C for 5 minutes between each coating cycle.

3. RESULT AND DISCUSSION

3.1 Structural Properties

3.1.1 XRD Analysis Results

Figure 1 shows the x-ray diffraction of ZnS and ZnS/Gr nanostructures. The comparison between pure ZnS has cubic zinc blende structure (pointed by * label) with a standard card ICDPDS (96-110-1051) was observed in Figure 1(a). The three main peaks of ZnS observed in the diffractogram at 2θ equal to 28.3549, 47.5354, and 56.195 corresponds to (111), (220) and (311) planes respectively. After the addition of Gr to ZnS, a new phase for ZnS appeared that is a hexagonal structure (pointed by # label) with a comparison to the standard card ASTM (I2-688) as shown in Figure 1(b). A new phase was formed because Gr sheet has hexagonal structure (honeycomb lattice), therefore, the graphene sheet becomes a template for ZnS growth. In the

same time, graphene peaks appeared at 2θ equal to 26.6351, 62.6492, and 67.7479 which corresponds to (002), (227), (416,228) planes respectively (pointed by @ label).
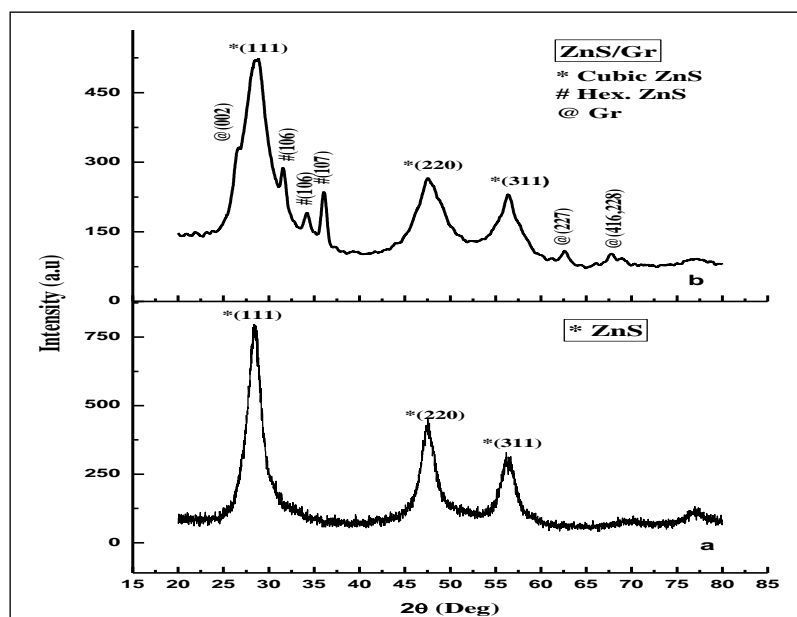

Figure 1. XRD patterns for ZnS and ZnS/Gr.

The average crystallite size is calculated from the Scherer formula [D=0.9λ/(β cosθ)] where λ is the x-ray wavelength (here λ = 1.54060 Å), θ is the Bragg angle, and β is the full-width at half-maximum (FWHM) measured in radian.

Table 1 Structural Parameters of ZnS and ZnS/Gr which are diffraction angle, (hkl), d-spacing, and FWHM

Sample	2θ (deg)	FWHM (Rad)	Plane (hkl)	D crystallite size	Phase	Card no.
ZnS	28.3549	0.043611	111	3.281995	Cubic	96-110-1051
	47.5354	0.034889	220	4.34635	Cubic	5-0566
	56.195	0.027911	311	5.636229	Cubic	96-110-1051
ZnS/Gr	26.6351	0.024422	002	5.839009	Gr	23-64
	28.6179	0.052333	111	2.736683	cubic	96-110-1051
	31.5314	0.020933	106	6.916823	Hex	I2-688
	34.1819	0.024422	106	5.944541	Hex	I2-688
	36.0635	0.017444	107	8.36634	Hex	I2-688
	47.5354	0.069778	220	2.173182	Cubic	5-0566
	56.3367	0.055822	311	2.820021	Cubic	96-110-1051
	62.6492	0.022678	227	7.163442	Gr	22-1069
	67.7479	0.017444	416,228	7.973054	Gr	22-1069

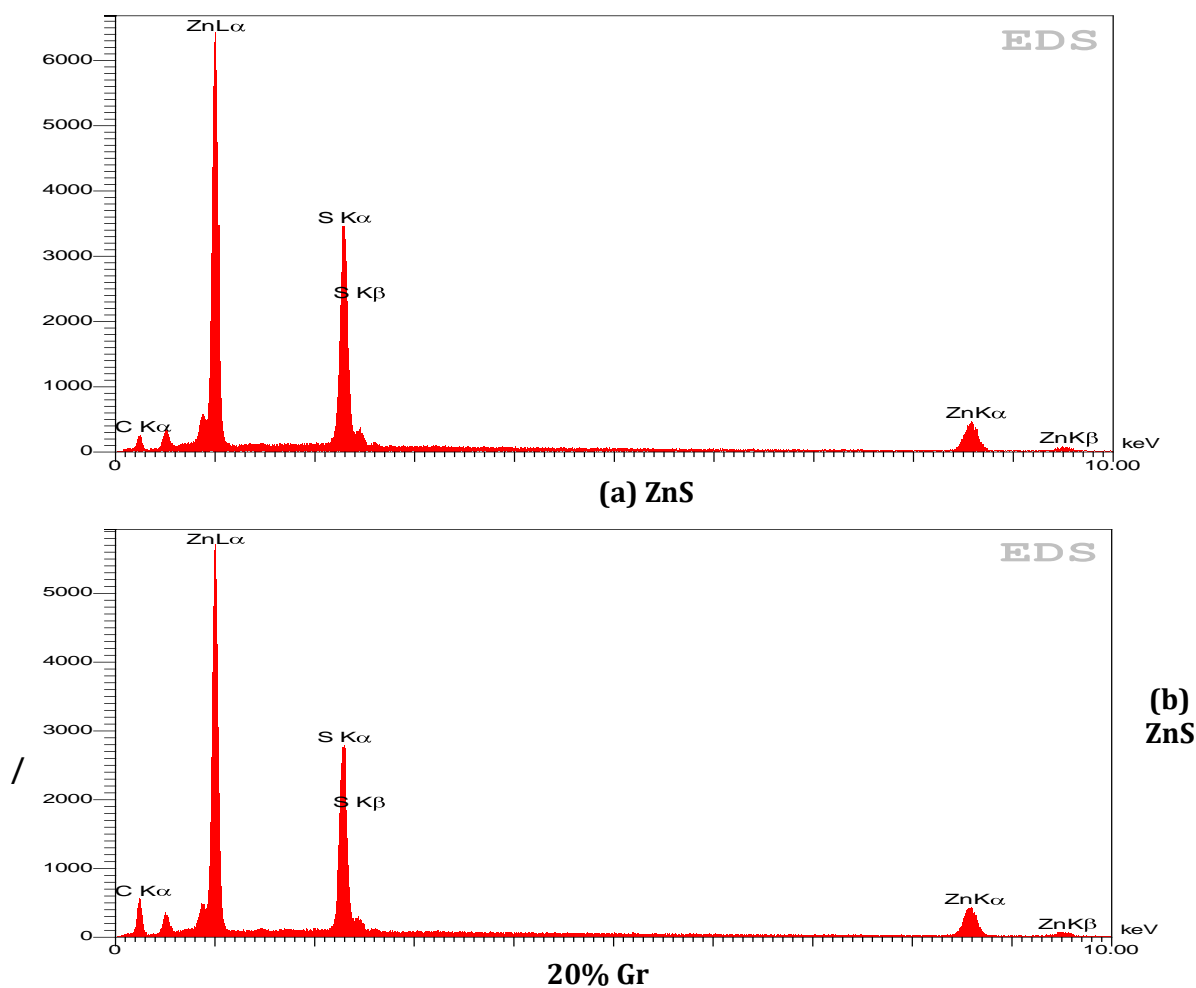### 3.1.2 EDS Analysis Results

(a) ZnS

(b) ZnS

20% Gr

Figure 2. EDS analysis for ZnS and ZnS/Gr.

Table 2 EDS measurements of ZnS/Gr system

Sample	Elements	Weight %	Atomic %	Series
ZnS	S	22.84	22.26	Kα
	Zn	57.92	27.69	Kα
ZnS/Gr	C	32.02	67.15	Kα
	S	16.63	13.06	Kα
	Zn	51.36	19.79	Kα

The chemical composition of pure ZnS and ZnS/Gr is shown in Figure 2(a) and 2(b). Table 2 illustrates the EDS results and shows the weight and atomic percentage of Zn, S and C. The Zn and S peaks depict the characteristic of the chemical composition of the synthesized nanomaterials. The results reveal that after Gr addition, the weight and atomic percentages of Zn and S reduce and increase for element C, hence, proved the formation of ZnS/ graphene system.

3.1.3 SEM Analysis Results

a) ZnS at low magnification

b) ZnS at high magnification

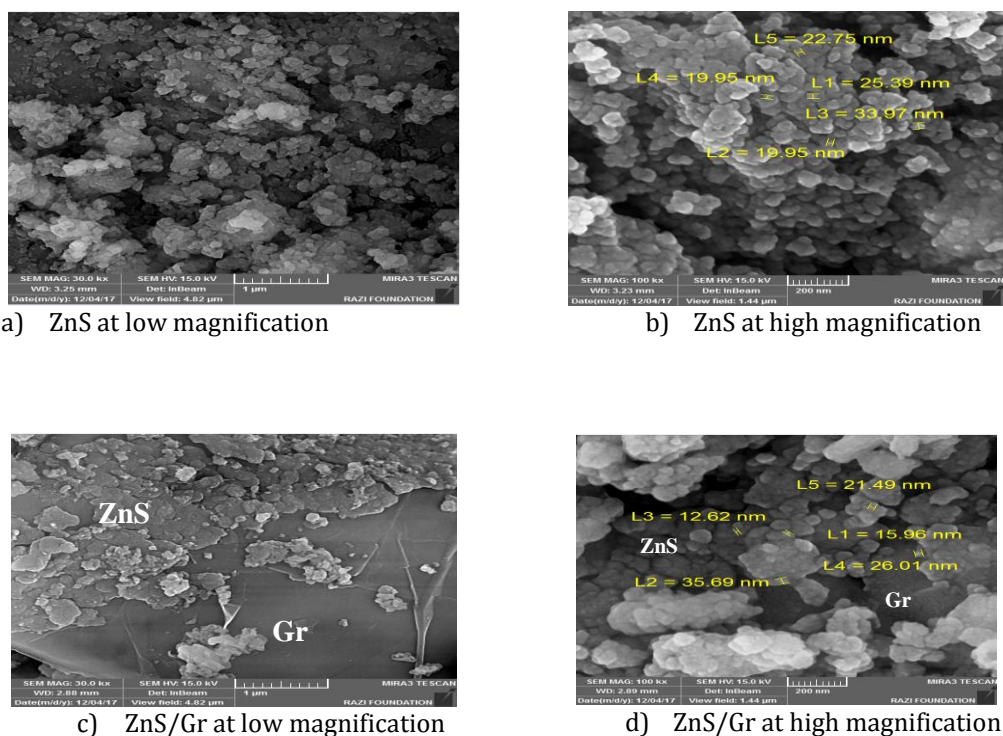c) ZnS/Gr at low magnification

d) ZnS/Gr at high magnification

Figure 3. SEM images of ZnS and ZnS/Gr.

SEM is a versatile technique for studying the morphology of materials. Figure 3(a) and 3(b) illustrate the images of pure ZnS prepared by co-precipitation route without adding the graphene that has nanosize with nanoparticle structure. The ZnS nanoparticles tend to aggregate without the dispersion of graphene. For ZnS/Gr, the interaction between the graphene and Zn^{2+} may be responsible for the uniform dispersion of ZnS nanoparticles on graphene. Figure 3(c) and 3(d) clearly show the ZnS nanoparticles loaded on graphene nanosheet.

3.2 Electrical Properties

3.2.1 I-V Characteristics for ZnS and ZnS/Gr

The type of electrical contact was investigated by plotting the I–V characteristics for ZnS and ZnS/Gr. The I–V curve in Figure 4 shows a non-linear behaviour indicating that the electrical contact is not ohmic. The I-V curve for ZnS has rectifier behaviour because the reverse current is still constant with a small value which equals to saturated current I_s and its rectifier factor calculated by the relation [rf=I_f/I_r] is ~30, which approaches ideal rectifier diode. For ZnS/Gr, the carriers transported easily because there is lower rectification than pure ZnS as in Figure 4.
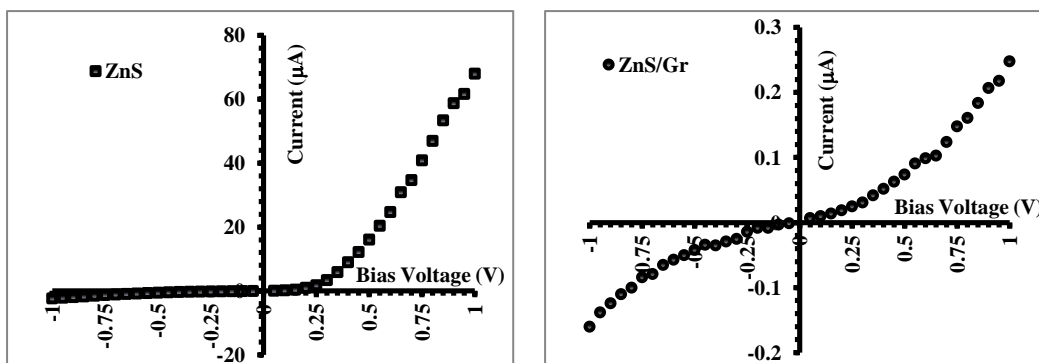
Figure 4. I-V characteristics in the dark for ZnS and ZnS/Gr.

In general, the forward dark current is generated due to the flow of majority carriers by the applied voltage which decreases the value of built-in potential and the width of the depletion layer. The majority and minority carrier concentration are higher than the intrinsic carrier concentration (ni2<np) which generate recombination current at the low voltage region (0-0.3V). The excitation electrons from valence band (V.B) to covalence band (C.B) will recombine with holes found in the V.B and this is observed by little increase in recombination current at low voltage region. The tunnelling current was represented at the high voltage region (>0.3V) where there is a fast exponential increase in the current magnitude with the increasing voltage and this is called diffusion current. The reverse bias current which also contains two regions, in the first region (low voltages<0.3V), the current slightly increases with the increasing applied voltage, and the generation current dominates. On the other hand, in the second region which is the high voltage region (>0.3V), the diffusion current dominates [15]. The value of saturation current I_s and idealistic factor n is calculated from this equation [$n = (q/k_BT)(V/Ln(I_f/I_s))$] where V and I_f is the forward bias voltage and forward current respectively, q is electronic charge, k_B is Boltzmann constant, and T is temperature which is 300K.

In forward bias, minority carriers are injected into quasi-neutral regions and these injected minority carriers recombine at the surface. In reverse bias, minority carriers are extracted from quasi-neutral regions where extracted minority carriers are generated at the surface.

Table 3 I_s, n and Φ_β for p-PS at different etching current densities in dark

Sample	n	Φ_β (eV)	I_s (μA)
ZnS	2.80	0.4377	1.79
ZnS/Gr	4.40	0.5540	0.02

From current-voltage measurements one can determine the potential barrier height (Φ_{Bn}) which can be determined by the relation [$\Phi_{Bn} = (k_BT/q)ln(AA*T^2/I_s)$] where A is the Schottky contact area which is 0.1485 cm^2, A* is the effective Richardson constant and I_s, n, Φ_{Bn} values are as tabulated in Table (3).

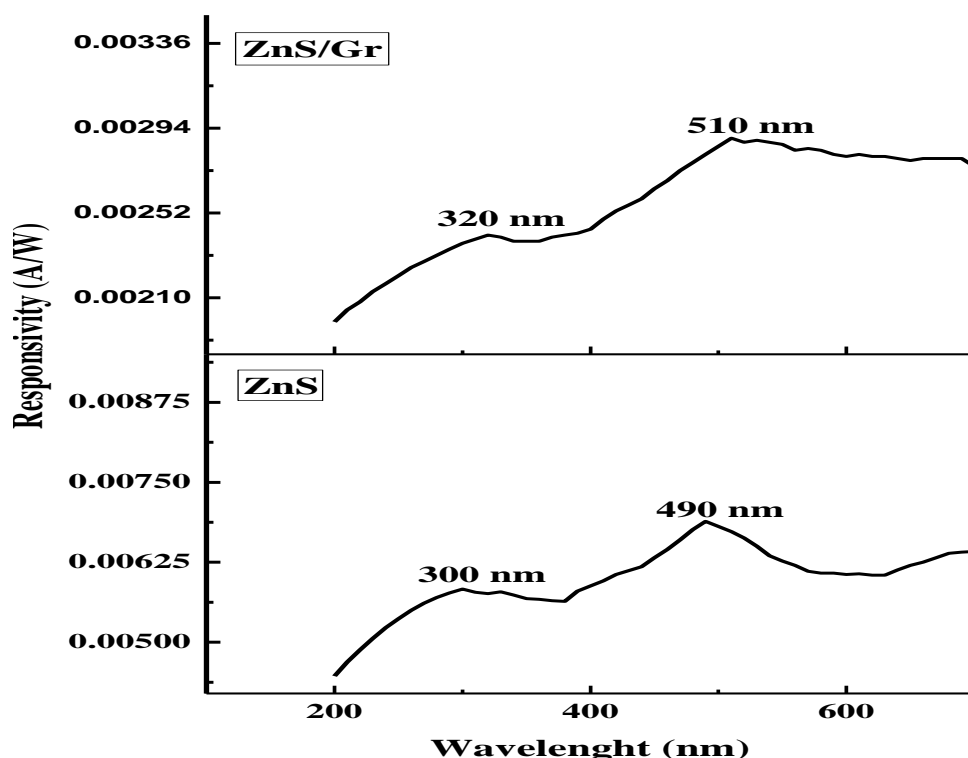### *3.2.2 Responsivity R_λ for ZnS and ZnS/Gr*

Figure 5. The variation of spectral responsivity of ZnS and ZnS/Gr as a function of the wavelength.

The light responsivity of the detector is measured in the wavelength range of 200–900 nm under zero bias voltage. Figure 5 shows the measured maximum values of responsivity and their values are in the UV region at 300 nm (for ZnS excitonic transition) and at 490 nm (for the transition of electrons between zinc vacancy acceptor level and sulphur vacancy donor level). Results observed in Figure 5 agree with Huaming *et al*. [15]. After graphene loading, there is redshift for these two peaks maxima which are at 320 nm for UV region and 510 nm for visible region. Therefore, ZnS nanoparticles can be tuned by functionalization with graphene nanosheet. In addition, there is a broad peak meaning that the material has a response for a wide range of wavelength.

Table 4 The values of spectral responsivity corresponding to maximum wavelength for ZnS and ZnS/Gr

Sample	Wavelength (nm)		Responsivity (A/W)	
ZnS	300	490	0.00583	0.00689
ZnS/Gr	320	510	0.00241	0.00289

4. CONCLUSIONS

ZnS/graphene nanostructure has been synthesized by a simple co-precipitation route. The ZnS nanoparticles with a size below 100 nm are uniformly loaded on the graphene sheets using Zn^{2+} as the precursor. The ZnS/graphene nanostructure exhibits improved optical and electrical properties compared to bare ZnS due to the incorporation of graphene which acts both as a buffer to alleviate the volume changes and as a separator to refrain the aggregating of the particles. Furthermore, the introduced graphene offers a conducting channel for ZnS and increases the specific surface area, enhancing the detection of visible wavelengths.

REFERENCES

[1]   R. Rossetti, J. L. Ellison, J. M. Gibson, L. E. Brus, J. Chem. Phys. **80** (1984) 4464.

[2]   K. Jayanthi, S. Chawla, H. Chander & D. Haranath, Structural, optical and photoluminescence properties of ZnS: Cu nanoparticle thin films as a function of dopant concentration and quantum confinement effect, Cryst. Res. Technol. **42**, 10 (2007) 976 – 982.

[3]   T. Ben Nasr, N. Kamoun, M. Kanzari, R. Bennaceur, Effect of pH on the properties of ZnS thin films grown by chemical bath deposition, Thin Solid Films, **500** (2006) 4-8**.**

[4]   B. L. Sharma, R. K. Purohit, "Semiconductors Heterojunctions", Academic Prees, Inc, Oxford, NewYork, (1974) 1-15.

[5]   G. Milnes & D. L. Feucht," Heterojunctions and Metal Semiconductors Junctions"Academic Prees, London, (1972).

[6]   Huang Jian, Wang Lin-Jun, Tang Ke, Xu Run, Zang Ji-Jun, Lu Xiong-Gang, Xia Yiben, Photoresponse Properties of an n-ZnS/p-Si Heterojunction**,** Chin. Phys. Lett. **28**, 12 (2011) 127301-3.

[7]   A. K. Geim & K. S. Novoselov, "The rise of graphene," Nature Materials **6** (2007) 183- 191.

[8]   L. Ponomarenko, F. Schedin, M. Katsnelson, R. Yang, E. Hill, K. Novoselov, *F.,* "Chaotic Dirac billiard in graphene quantum dots," Science **320** (2008) 356-358.

[9]   F. Schedin, A. Geim, S. Morozov, E. Hill, P. Blake, M. Katsnelson, *et al.,* "Detection of individual gas molecules adsorbed on graphene," Nature Materials **6** (2007) 652-655.

[10] Y. Zhou, J. Zhang, D. Zhang, C. Ye & X. Miao, "Phosphorus-doping-induced rectifying behavior in armchair graphene nanoribbons devices," Journal of Applied Physics **115** (2014) 013705.

[11] Callister J. & Malinowski S., "Optical Properties In Anderson", Materials Science and Engineering: An Introduction (6th). John Wiley & Sons, Inc.: New Jersey, (2003) 707–729.

[12] Mishra S. K., Srivastava R. K., Prakash S. G., Yadav R. S. & Panday A. C., "Photoluminescence and photoconductive characteristics of hydrothermally synthesized ZnO nanoparticles", Opto−Electronics Rev. **18** (2010) 467.

[13] Eman M. N., "Fabrication and Characterization of n-ZnS/p-Si and n-ZnS:Al/p-Si Heterojunction", Int. J. Engineering and Advanced Technology, **3**, 2 (2013).

[14] Law J. B. & Thong J. T., "Simple fabrication of a ZnO nanowire photodetector with a fast photoresponse time", Appl. Phys. Lett. **88** (2006) 133114.

[15] Huaming Y., Chenghuan H., Xiaohui S. & Aidong T., "Microwave-assisted synthesis and luminescent properties of pure and doped ZnS nanoparticles", J. of Alloys and Compounds **402** (2005) 274–277.